Proc. Natl. Acad. Sci. USA
Vol. 80, pp. 983–987, February 1983
Biophysics

Energetics of photosynthetic glow peaks

(thermoluminescence/delayed light/reversed electron flow/electron and hole traps)

DON DEVAULT*, GOVINDJEE*†, AND WILLIAM ARNOLD§

Departments of *Physiology and Biophysics and †Botany, University of Illinois at Urbana-Champaign, Urbana, Illinois 61801; and §Department of Biology, Oak Ridge National Laboratory, Oak Ridge, Tennessee 37830

Contributed by William Arnold, November 5, 1982

ABSTRACT **By postulating temperature-dependent equilibria between two or more electron carriers acting as traps for electrons or holes, it is possible to modify the Randall–Wilkins theory of thermoluminescence so as to explain the abnormally large apparent activation energies and apparent frequency factors observed in photosynthetic glow curves when fitted by unmodified Randall–Wilkins theory. The equilibria serve to inhibit the formation of the light-emitting excited state by withholding the needed precursor state. When the inhibition is released at higher temperature by shift of equilibrium with temperature, the rise of the glow peak can be much faster than would result from Arrhenius behavior based on the true activation energy and so appears to correspond to a higher activation energy accompanied by a larger frequency factor. From another viewpoint, the enthalpy changes, ΔH, of the equilibria tend to add to the activation energy. Similarly the entropy changes, ΔS, of the equilibria tend to add to the entropy of activation, giving the large apparent frequency factors. The positive values of ΔS needed would correspond to entropy decreases in the forward early electron transport. A comparison of the glow peaks obtained by different workers is also presented.**

Photosynthetic materials frozen in liquid nitrogen while illuminated emit thermoluminescence when warmed in the dark at a constant rate (1, 2). Curves of the intensity of emitted light vs. temperature show a series of characteristic peaks. The lowest temperature peak from chloroplasts and algal cells, called "Z," appears to have nothing to do with photosynthesis. Five other peaks have been labeled "I" to "V" by Desai *et al.* (3) and "Zv," "A," "B_1," "B_2," and "C" by Ichikawa *et al.* (4). Demeter and co-workers (5, 6) added two more peaks and labeled them with their approximate Celsius temperatures. Correspondence between these labeling systems will be discussed later.

Tatake *et al.* (7) analyzed these peaks, attempting to fit them to the Randall–Wilkins (8) theory. This theory assumes, simply, that the thermoluminescence arises from electrons trapped in metastable states when they manage to free themselves and migrate to a location that will bind the electron more stably, emitting light in the process. It further assumes that the rate of detrapping can be expressed by an Arrhenius equation:

$$I = -\phi \frac{dn}{dt} = \phi n k = \phi n s e^{-E/k_B T} \qquad [1]$$

where I is the intensity of glow, ϕ is a proportionality constant, n is the number of trapped electrons, k is the reaction rate constant, s is a preexponential frequency factor (the rate at infinite temperature by extrapolation according to Arrhenius theory), E is the activation energy, k_B is Boltzmann's constant, and T is the absolute temperature. Vass *et al.* (6) substitute $s_0 T$ for s in order to agree with absolute reaction rate theory. The additional dependence of rate on T is minor compared to the exponential dependence and probably does not make appreciable practical difference, compared, say, to our neglect of any dependence of E on T.

The integrated equation can be expressed as

$$I = \phi n_0 s \exp\left(-\frac{E}{k_B T} - \frac{s}{B} \int_{T_0}^{T} e^{-E/k_B T} dT \right), \qquad [2]$$

where B is the rate of heating and n_0 is the number of trapped electrons at T_0. The initial integration limit, T_0, may be set equal to zero if, as is usual, the glow curve starts at such a low temperature that the initial rate v of detrapping is negligibly small. Eq. 2 with constant values for all quantities except T and I describes a single peaked curve with the temperature, T_m, at the peak. The preexponential frequency factor is related to T_m, E, and B by

$$s = \frac{BE}{k_B T_m^2} \exp(E/k_B T_m). \qquad [3]$$

The various peaks presumably result from different groups of trapped electrons whose detrapping involves different values of the parameters.

Some of the results of analysis by Tatake *et al.* (7) are shown in Table 1. We have added the column labeled $\Delta S^{\ddagger}/k_B$, which represents the entropy of activation divided by the Boltzmann constant, corresponding to the value of s in the previous column calculated according to absolute reaction rate theory by the formula

$$\Delta S^{\ddagger}/k_B = \ln(sh/k_B T_m), \qquad [4]$$

where ln is the natural logarithm, h is Planck's constant, and T_m is used as an average temperature for the curve of a single glow peak. Values much larger than zero for activation entropies are suspect. The extremely large values of s and $\Delta S^{\ddagger}/k_B$ for peaks IV and V appear to be impossibly large. One does not expect positive values for $\Delta S^{\ddagger}$ because the activated state is presumed to be a restricted, specialized state with lower entropy than that of the reactants forming it. Values of s larger than 10^{13} sec^{-1} are outside the range of chemical reaction kinetics; 10^{15} sec^{-1} corresponds to electronic vibrations in the valence shells of atoms and 10^{19} sec^{-1} to a 50,000 eV quantum. Tatake *et al.* (7) concluded that peaks IV and V do not follow Randall–Wilkins theory.

The method of analysis used by Tatake *et al.* used only the early part of the rising portion of a glow peak and the peak point. We reanalyzed the data with a computer match to the whole curve. Despite some differences, we agree with the general picture presented by Table 1. A preliminary report has been made (9). Since then the paper of Vass *et al.* (6) appeared. Their s_0 values must be multiplied by T_m to correspond to our s and, despite

---

The publication costs of this article were defrayed in part by page charge payment. This article must therefore be hereby marked "*advertisement*" in accordance with 18 U. S. C. §1734 solely to indicate this fact.

Abbreviation: DCMU, 3-(3′,4′-dichlorophenyl)-1,1-dimethylurea.

Table 1. Photosynthetic glow peak parameters resulting from fitting with Randall–Wilkins theory*

Glow peak	Glow curve	T_m, K	E, eV	s sec^{-1}	$\Delta S^{\ddagger}/k_B$
I	1	236	0.52	2.5×10^9	−7.6
II	2	261	0.64	4.5×10^{10}	−4.8
III	2	283	0.79	2.4×10^{12}	−0.9
IV	1	298	1.10	1.0×10^{17}	9.7
V	3	321	1.32	1.4×10^{19}	14.6

* By Tatake *et al.* (7). Glow curve 1 was taken from untreated spinach chloropasts frozen in the presence of intense white light. Glow curve 2 differed only in being pretreated with 3-3′,4′-dichlorophenyl-1,1-dimethylurea (DCMU). Glow curve 3 was from Euglena cells illuminated and then relaxed in the dark at room temperature 5 min before being frozen. The glow curve numbers correspond to the figure numbers displaying the curves in Tatake *et al.* (7).

some discrepancies, also appear too large, especially in the peaks "+30" and "+45" corresponding to peaks IV and V.

PROPOSED THEORY

We assume that thermoluminescence is a reversal of light-induced electron transport as also proposed by many to explain "delayed light." (For reviews on delayed light, see refs. 10–13.) Fig. 1 shows the required electron flow in the reverse direction through two reaction centers P_{680} and P_{700}. We assume that the light is emitted from the first excited singlet state of antenna chlorophyll to which the excitation was transferred after being created in the reaction center chlorophyll. The latter is obtained by migration to it of a hole from where it was trapped (in one of the carriers) on the donor side and of an electron from where it was trapped (in one of the carriers) on the acceptor side. Therefore, it could require several steps instead of the single step postulated by the Randall–Wilkins theory.

Our proposal is that the kinetics of the detrapping may involve not only the rate-limiting step but also earlier steps. Because they will be faster, we assume most simply that they reach equilibria. They affect the rate by governing the concentration of carriers that are ready for the rate-determining step. The equilibria will shift with temperature according to the enthalpy changes involved. As the inhibition lifts at a higher temperature, the glow will rise more rapidly than it would have done without the inhibition and will appear to have higher E and s or $\Delta S^{\ddagger}/k_B$ values. Thus, Eq. 1 is modified by multiplying its right side by the fraction of carriers ready for the rate-determining step:

$$I = -\phi \frac{dn}{dt} = \phi n\, F(T) \qquad [5]$$

where $F(T)$ is k, the rate constant for the rate-determining step, times the fraction of carriers ready for it. The form of $F(T)$ is listed in Table 2 for four likely mechanisms, including Randall–Wilkins as mechanism I.

The full dependence of F on temperature is shown in Table 2 by writing the rate constants as $(k_B T_m/h)\exp(\Delta S^{\ddagger}/k_B)\exp(-E/k_B T)$ and expanding the equilibrium constants, K, in terms of the entropy change, ΔS, and the enthalpy change, ΔH, of each equilibrium reaction:

$$K = e^{-\Delta G/k_B T} = e^{\Delta S/k_B}\, e^{-\Delta H/k_B T}. \qquad [6]$$

The integrated form of Eq. 5 is:

$$I = \phi n_0 F(T) \exp\left[-\frac{1}{B}\int_{T_0}^{T} F(T)dT\right]. \qquad [7]$$

The temperature of the peak can be found by solving the following equation

$$dF(T_m)/dT_m = [F(T_m)]^2/B \qquad [8]$$

for T_m.

As an example we calculate a hypothetical case of mechanism II. This mechanism may be written:

$$A \leftrightarrow B \overset{\star}{\rightarrow} X + h\nu. \qquad [9]$$

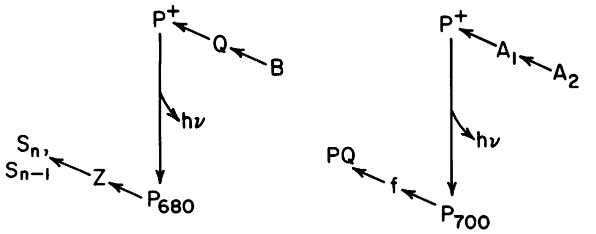

FIG. 1. Electron carries near the reaction centers which could trap electrons (or holes). Arrows show reversed electron flow necessary to produce excitation (hν) in the reaction center which can migrate to antenna chlorophyll and produce fluorescence. Electron movement away from the reaction center to its left can be interpreted also as hole movement toward the center. S_n, state of the oxygen-evolving system; Z, electron donor to P_{680}; P_{680}(P), reaction center chlorophyll *a* of PS II; Q, primary quinone acceptor of PS II; B, secondary quinone acceptor of PS II; PQ, plastoquinone pool, designated Pq in Table 4; f, all electron donors to P_{700}, including plastocyanin (PC), Rieske Fe–S center, and cytochrome *f*; P_{700}, reaction center chlorophyll *a* of PS I; A_1 and A_2, first and secondary electron acceptors of PS I; PS I, photosystem I; and PS II, photosystem II.

Table 2. Some possible mechanisms and appropriate formulas

Mechanism	States	Formulas for substitution into Eqs. 5, 7, 8, and 10
I	A $\downarrow\ \star$	$n = [A]$ $F(T) = k = se^{-E/k_B T} = (k_B T/h)\, e^{\Delta S^{\ddagger}/k_B}\, e^{-E/k_B T}$ (Randall–Wilkins)
II	A $\updownarrow\ 1$ B $\downarrow\ \star$	$n = [A] + [B] = [A](1 + K_1)$ $F(T) = kK_1/(1 + K_1)$ $= \left(\frac{k_B T}{h}\right) \cdot \frac{e^{(\Delta S^{\ddagger}+\Delta S_1)/k_B}\, e^{-(E+\Delta H_1)/k_B T}}{1 + e^{\Delta S_1/k_B}\, e^{-\Delta H_1/k_B T}}$
III	A $\updownarrow\ 2$ B $\updownarrow\ 1$ C $\downarrow\ \star$	$n = [A] + [B] + [C] = [A](1 + K_2 + K_1K_2)$ $F(T) = kK_1K_2/(1 + K_2 + K_1K_2)$ $= (k_B T/h)\cdot(\text{num}/\text{den})$, where: $\text{num} = e^{(\Delta S^{\ddagger}+\Delta S_2+\Delta S_1)/k_B}\, e^{-(E+\Delta H_2+\Delta H_1)/k_B T}$ $\text{den} = 1 + e^{\Delta S_2/k_B}\, e^{-\Delta H_2/k_B T} + e^{(\Delta S_2+\Delta S_1)/k_B}\, e^{-(\Delta H_2+\Delta H_1)/k_B T}$
IV	A ^{3}⤢ ⤡^{2} C B ^{4}⤡ ⤢$_{1}$ D $\downarrow\ \star$	$n = [A] + [B] + [C] + [D]$ $= [A](1 + K_2 + K_3 + K_1K_2)$ $F(T) = kK_1K_2/(1 + K_2 + K_3 + K_1K_2)$ $= (k_B T/h) \cdot (\text{num}/\text{den})$, where: $\text{num} = e^{(\Delta S^{\ddagger}+\Delta S_1+\Delta S_2)/k_B}\, e^{-(E+\Delta H_1+\Delta H_2)/k_B T}$ $\text{den} = 1 + e^{\Delta S_2/k_B}\, e^{-\Delta H_2/k_B T} + e^{\Delta S_3/k_B}\, e^{-\Delta H_3/k_B T} + e^{(\Delta S_1+\Delta S_2)/k_B}\, e^{-(\Delta H_1+\Delta H_2)/k_B T}$.

$\star$, The rate-limiting step. Subscripts refer to numbers designating the equilibria in the successive states column. In all cases one gets the low-temperature approximation by assuming that all ΔH_is are positive, so that at a low enough temperature, the denominators of $F(T)$ approach 1 and the numerators become the low-temperature asymptotes. In the formulas, k is the rate constant of the rate-limiting step and Ks are equilibrium constants. In mechanism IV, $K_4 = K_1K_2/K_3$.

The star indicates the rate-limiting step and the double-headed arrow indicates the preceding equilibrium. The total concentration of trapped electron-hole pairs, n, is [A] + [B], the sum of the molar concentrations of trapped states designated A and B. The equilibrium constant, K, is equal to [B]/[A]. Thus, the fraction of states ready for the rate-limiting step is $[B]/n$ or $K/(1 + K)$.

The following reasonable parameters were chosen for the rate-limiting step: activation energy, $E = 0.6$ eV; frequency factor, $s = 9.62 \times 10^{10}$ sec^{-1} (gives $T_m = 240$ K and $\Delta S^{\ddagger}/k_B = -3.95$); and the rate of heating, $B = 0.2$ deg sec^{-1}. In Eq. 6, ΔS can be replaced by $\Delta H/T_E$ where T_E is the temperature at which $\Delta G = 0$ or [A] = [B]. T_E thus gives an idea of the temperature around which the inhibition is gradually lifted. For our example we chose $\Delta H = 0.6$ eV and five different values for T_E. In the case of $T_E = 0$ K, the equilibrium between A and B is always all B and no A, so there is no inhibition, and the result is Randall–Wilkins behavior.

The calculation was done by numerical integration of Eq. 7. The results are presented graphically in Figs. 2 and 3 and numerically in Table 3. Fig. 2 illustrates how the equilibrium delays the rise of the glow peak. It is seen that if the inhibition release temperature, T_E, is appreciably less than 240 K (the temperature of the peak with no inhibition), there is very little inhibition.

The factor in Eq. 7 containing the integral has to do with the depletion of the traps, so at temperatures appreciably below the peak where depletion is not yet important, we have the rising edge given approximately by

$$I_{(\text{rising edge})} \simeq \phi n_0 F(T). \qquad [10]$$

Assuming that the ΔHs are positive, the denominator of $F(T)$ (see Table 2) approaches 1 at low enough temperatures. Thus, for the early part of the rising edges, $F(T)$ is approximated by its numerator. Comparison of the numerators of $F(T)$ in Table 2 shows that $\Delta S^{\ddagger}$ in (Randall–Wilkins) mechanism I is augmented by simple addition of the ΔSs of the equilibria in the other mechanisms, and E, by the ΔHs. Thus, an Arrhenius plot of this early part of the rising portion of the glow peak would give an *apparent* activation energy approaching $(E + \Sigma\, \Delta H_i)$ and an *apparent* activation entropy approaching $(\Delta S^{\ddagger} + \Sigma\, \Delta S_i)$.

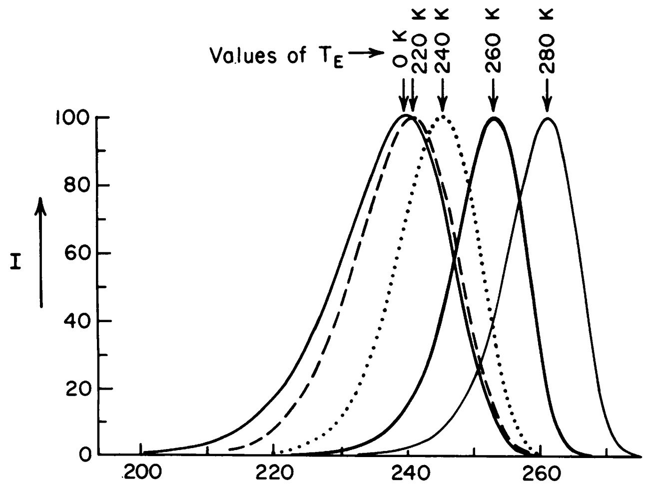

FIG. 2. Glow curves calculated by Eq. 7. Parameters are given in Table 3. T_E is the approximate temperature (K) around which the inhibition of the temperature-dependent equilibrium is released. Thus, $T_E = 0$ corresponds to no inhibition, in which case the curve follows Randall–Wilkins theory and peaks at 240°C. Any value of T_E less than 240 K exerts very little inhibition.

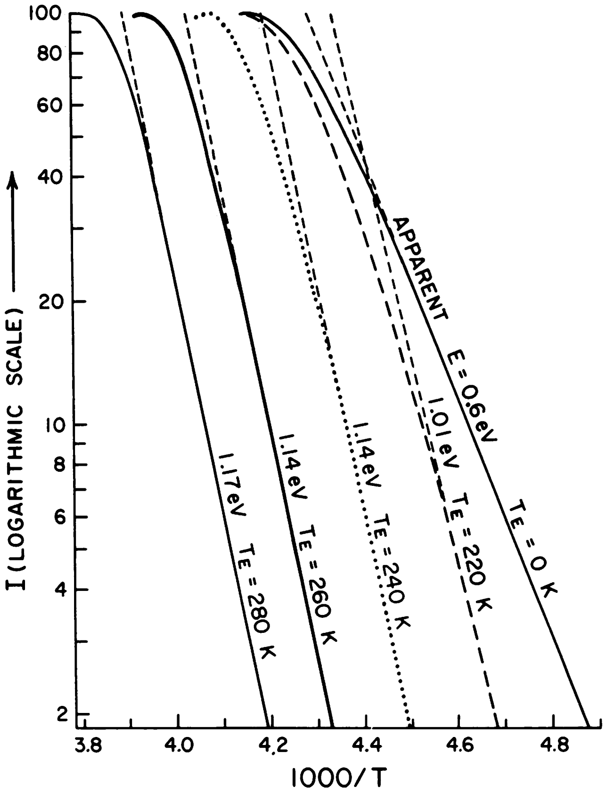

FIG. 3. Arrhenius plots of the rising portions of the curves of Fig. 2.

Fig. 3 is an Arrhenius plot of the rising portions of the curves in Fig. 2 and shows how the apparent activation energy approaches $E + \Delta H$ as the inhibition is made stronger. The apparent E values and the corresponding apparent s and apparent $\Delta S^{\ddagger}/k_B$ values are shown in Table 3. It is seen that the proposed mechanism can easily explain unreasonably high apparent values with reasonable actual values. It also is seen how the apparent E values approach 1.2 eV, the sum of E and ΔH, and the apparent $\Delta S^{\ddagger}/k_B$ approaches the actual $(\Delta S^{\ddagger} + \Delta S)/k_B$ as one goes from top to bottom of the table.

Demeter *et al.* (5) and Vass *et al.* (6) on the basis of the large values of E also conclude that thermoluminescence involves reversal of electron transport steps beyond the primary step, but they, like others before them, treat the whole reversal as a single step with additive energies. They do not explicitly address the problem of large frequency factors. The development above expresses all this more quantitatively.

Table 3. Apparent parameters resulting from prefixing an equilibrium before the detrapping step*

			Apparent values			Actual
T_E, K	$\Delta S/k_B$	T_m, K	E, eV	s, sec^{-1}	$\frac{\Delta S^{\ddagger}}{k_B}$	$\frac{\Delta S + \Delta S^{\ddagger}}{k_B}$
0	—	240.0	0.6	9.62×10^{10}	−3.95	−3.95
220	31.65	240.8	1.007	4.85×10^{19}	16.08	27.70
230	30.27	242.7	1.096	2.51×10^{21}	20.02	26.32
240	29.01	245.8	1.137	9.03×10^{21}	21.29	25.06
260	26.78	253.4	1.144	2.30×10^{22}	19.89	22.83
280	24.87	261.3	1.167	1.29×10^{22}	19.28	20.92

* Values are derived from the curves of Figs. 2 and 3. In all cases: $E = 0.6$ eV, $\Delta H = 0.6$ eV, $s = 9.62 \times 10^{10}$ sec^{-1}, $\Delta S^{\ddagger}/k_B = -3.95$. Mechanism II of Table 2 was assumed.

EXAMPLES OF POSSIBLE APPLICATIONS

Fig. 4 shows a comparison of the glow peaks obtained by various workers with different rates of heating. With three exceptions, we see only DCMU inhibited peaks to the left of the 255 K dashed line and between the 287 K and 311 K lines. With possibly three exceptions, we see only peaks not inhibited by DCMU between the 255 K and 287 K lines and to the right of the 311 K line. We suggest that these lines group the peaks of different workers that are equivalent.

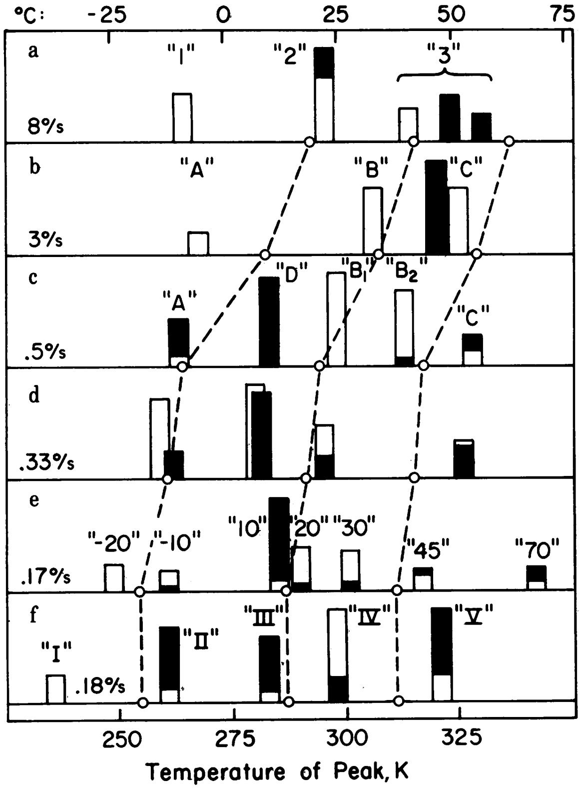

FIG. 4. Comparison of glow peaks reported by different groups of workers. The bar graphs show peak positions reported by them. The top of a white section of bar indicates the amplitude without DCMU present, and the top of a black section of bar, the amplitude with DCMU, both with respect to the base-line for the total bar. Thus, a white-topped bar indicates a peak inhibited by DCMU, and a black-topped bar, a peak not inhibited by DCMU. (*a*) Data from ref. 14 (see figure 3 there). (*b*) Data from ref. 15 plus notes of one of us (W.A.). (*c*) Data from ref. 4 (see figure 4 there). (*d*) Data from ref. 16. (*e*) Data from ref. 6 (see figures 2 and 5A there). (*f*) Data from ref. 7. ----, Positions expected according to Eq. 3 for hypothetical peaks assumed to be at 255, 287, and 311 K, respectively, when the heating rate is 0.18°C sec^{-1}. In calculating them, the activation energy E was assumed to be 0.6 eV, 1.0 eV, and 1.3 eV, respectively, the heating rates [°C/sec(s)] were assumed to be as indicated for the different glow curves, and s was assumed to be constant for each line.

Most authors in the field of photosynthetic thermoluminescence have attempted assignments of origin of glow peaks to various parts of the photosynthetic system (2, 4, 6, 14–20). Inoue and Shibata (21) have reviewed the details. Based on this research, we suggest some speculative assignments in order to illustrate possible application of the mechanisms proposed here (Table 4).

Table 4. Working hypotheses for assignment of glow peaks to reactions in photosynthesis

Glow peak	Table 2 mech.	Possible assignment of trapping states listed in Table 2			
		A	*B*	*C*	*D*
I	I	$S_4P_{680}Q^{-}$*			
	II	$S_4P_{680}Q^{-}$*	$S_3P^+Q^-$		
II	II	$S_3P_{680}Q^-$	$S_2P^+Q^-$		
	III	$S_3ZP_{680}Q^-$	$S_2Z^+PQ^-$	$S_2ZP^+Q^-$	
(II-DCMU)	I	$S_2P_{680}Q^-$			
	II	$S_2P_{680}Q^-$	$S_1P^+Q^-$		
III	II	$S_2P_{680}Q^-$	$S_1P^+Q^-$		
	III	$S_2ZP_{680}Q^-$	$S_1Z^+PQ^-$	$S_1ZP^+Q^-$	
IV	II	$f^+P_{700}A_1^-$	$fP^+A_1^-$		
	IV	$S_2P_{680}QB^{-}$†	S_2PQ^-B	$S_2P^+QB^-$	$S_2P^+Q^-B$
V	III	$Pq^+fP_{700}A_1^-$	$Pqf^+PA_1^-$	$PqfP^+A_1^-$	
	IV	$f^+P_{700}A_1A_2^-$	$f^+PA_1^-A_2$	$fP^+A_1A_2^-$	$fP^+A_1^-A_2$

For the meaning of symbols, see the legend of Fig. 1.

* However, see refs. 3 and 18 for alternate views.

† See ref. 19 for a similar suggestion for peak B_1.

CONCLUDING REMARKS

Large positive values of ΔS for the equilibrium reactions, discussed in this paper, may be reasonable in the light of the finding (22–24) that, in the bacterial systems, there is a large decrease in entropy in the forward movement of electrons through the reaction center such that ΔG stored 1 msec after absorption of a photon is almost entirely $-T\Delta S$. The value of this $\Delta S/k_B$ is about -30 per electron. Thus, in the reversal of these reactions as in thermoluminescence, one might expect $\Delta S/k_B$ to go as high as $+30$. On the other hand, other data from experiments on delayed fluorescence (25, 26) contradict the large entropy changes.

Not considered in the mechanisms of Table 2 is the possibility of competing parallel reactions for detrapping the same traps by a pathway that does not lead to fluorescence (or has a different efficiency factor), (cf. ref. 27).

Especially valuable in future research would be simultaneous spectrophotometric measurement of the components thought to be involved in thermoluminescence. More measurements of the characteristics of the components of the photosynthetic system and of the electron transport reactions between them are necessary, including not only more equilibrium data but also, importantly, their temperature dependence. In other words, we need ΔHs or ΔSs as well as ΔGs.

Fitting parameters to glow curves is a difficult way to measure the parameters. Constant temperature measurements of the kinetics of thermoluminescence would be less complicated to interpret. One could, for example, prepare a sample as for a glow curve, but instead of warming it at a constant rate in the dark, one could produce a fast temperature jump to a specific temperature of interest concerning a particular glow peak and then hold the temperature constant while observing the kinetics of the light emission (see e.g., refs. 6, 28, and 29). At temperatures where a glow curve would show overlapping peaks, one could expect to find biphasic kinetics. Vass *et al.* (6) criticize the temperature-jump method as difficult to interpret because of the multiple phases. It appears that either method can require the sorting out of multiple components, but the parameters of the components are more directly determined in the temperature-jump method.

We thank Dr. V. G. Tatake and his group for letting us use their original data. Financial aid was received from the National Science Foundation (Grants PCM 78-23194 and PCM 81-09854) and from a Biomedical Research Support Grant administered by the University of Illinois.

1. Arnold, W. & Sherwood, H. (1957) *Proc. Natl. Acad. Sci. USA* **43**, 105–114.
2. Arnold, W. & Azzi, J. R. (1968) *Proc. Natl. Acad. Sci. USA* **61**, 29–35.

3. Desai, T. S., Sane, P. V. & Tatake, V. G. (1975) *Photochem. Photobiol.* **21**, 345–350.
4. Ichikawa, T., Inoue, Y. & Shibata, K. (1975) *Biochim. Biophys. Acta* **408**, 228–239.
5. Demeter, S., Vass, I., Herczeg, T., Droppa, M. & Horvath, G. (1981) in *Photosynthesis I: Photophysical Processes Membrane Energization*, ed. G. Akoyunoglou (Balaban International Science Service, Philadelphia), pp. 655–663.
6. Vass, I., Horvath, G., Herczeg, T. & Demeter, S. (1981) *Biochim. Biophys. Acta* **634**, 140–152.
7. Tatake, V. G., Desai, T. S., Govindjee & Sane, P. V. (1981) *Photochem. Photobiol.* **33**, 243–250.
8. Randall, J. T. & Wilkins, M. H. F. (1945) *Proc. R. Soc. London Ser. A* **184**, 366–389.
9. DeVault, D., Govindjee & Arnold, W. (1981) *Biophys. J.* **33**, 18 (abstr. M-AM-E1).
10. Lavorel, J. (1975) in *Bioenergetics in Photosynthesis*, ed. Govindjee (Academic, New York), pp. 233–317.
11. Malkin, S. (1977) in *Photosynthesis I.*, eds. Trebst, A. & Avron, M. (Springer, Berlin), pp. 473–491.
12. Malkin, S. (1977) *Top. Photosynthesis* **2**, 349–431.
13. Govindjee & Jursinic, P. (1979) *Photochem. Photobiol. Rev.* **4**, 125–205.
14. Lurie, S. & Bertsch, W. (1974) *Biochim. Biophys. Acta* **357**, 420–428.
15. Arnold, W. & Azzi, J. R. (1971) *Photochem. Photobiol.* **14**, 233–240.
16. Rubin, A. B. & Venediktov, P. S. (1969) *Biofizika* **14**, 105–109.
17. Shuvalov, V. A. & Litvin, F. F. (1969) *Mol. Biol. (Kiev)* **3**, 59–73.
18. Sane, P. V., Desai, T. S., Tatake, V. G. & Govindjee (1977) *Photochem. Photobiol.* **26**, 33–39.
19. Rutherford, A. W., Inoue, Y. & Crofts, A. R. (1982) *Biochim. Biophys. Acta*, in press.
20. Inoue, Y. (1981) *Biochim. Biophys. Acta* **634**, 309–320.
21. Inoue, Y. & Shibata, K. (1982) in *Photosynthesis I. Energy Conversion by Plants and Bacteria*, ed. Govindjee (Academic, New York), pp. 507–533.
22. Callis, J. B., Parson, W. W. & Gouterman, M. (1972) *Biochim. Biophys. Acta* **267**, 348–362.
23. Case, G. D. & Parson, W. W. (1971) *Biochim. Biophys. Acta* **253**, 187–202.
24. Arata, H. & Parson, W. W. (1981) *Biochim. Biophys. Acta* **636**, 70–81.
25. Carithers, R. P. & Parson, W. W. (1975) *Biochim. Biophys. Acta* **387**, 194–211.
26. Arata, H. & Parson, W. W. (1981) *Biochim. Biophys. Acta* **638**, 201–209.
27. Fleischman, D. E. (1971) *Photochem. Photobiol.* **14**, 65–70.
28. Mar, T. & Govindjee (1971) *Biochim. Biophys. Acta* **226**, 200–203.
29. Malkin, S. & Hardt, H. (1973) *Biochim. Biophys. Acta* **305**, 292–301.